Supporting Information for:

Rapid Characterization of Formulated Pharmaceuticals Using Fast MAS ^{1}H Solid-State NMR Spectroscopy

David A. Hirsh,[1#] Anuradha V. Wijesekara,[1#] Scott L. Carnahan,[1] Ivan Hung,[2] Joseph W. Lubach,[3*] Karthik Nagapudi,[3*] and Aaron J. Rossini,[1*]

[1]Iowa State University, Department of Chemistry, Ames, IA, USA, 50011

[2]Center of Interdisciplinary Magnetic Resonance, National High Magnetic Field Laboratory, 1800 East Paul Dirac Drive, Tallahassee, FL 32310, USA.

[3]Genentech Inc., South San Francisco, CA, USA, 94080

* Authors to whom correspondence should be addressed:
A.J.R. E-mail: arossini@iastate.edu
J.W.L E-mail: lubach.joseph@gene.com
K.N. E-mail: nagapudi.karthik@gene.com

Table of Contents

Supplementary Figures and Tables

Table S1. Dosage and the API loading of the commercial tablets used in the study.

Commercial Tablet	Dosage/(mg)	Mass of a tablet/(mg)	API loading/ (w/w %)
Mecl	25.0	201.3	12.4
Phenaz	97.5	143.2	68.1
Pheny	10.0	141.5	7.1

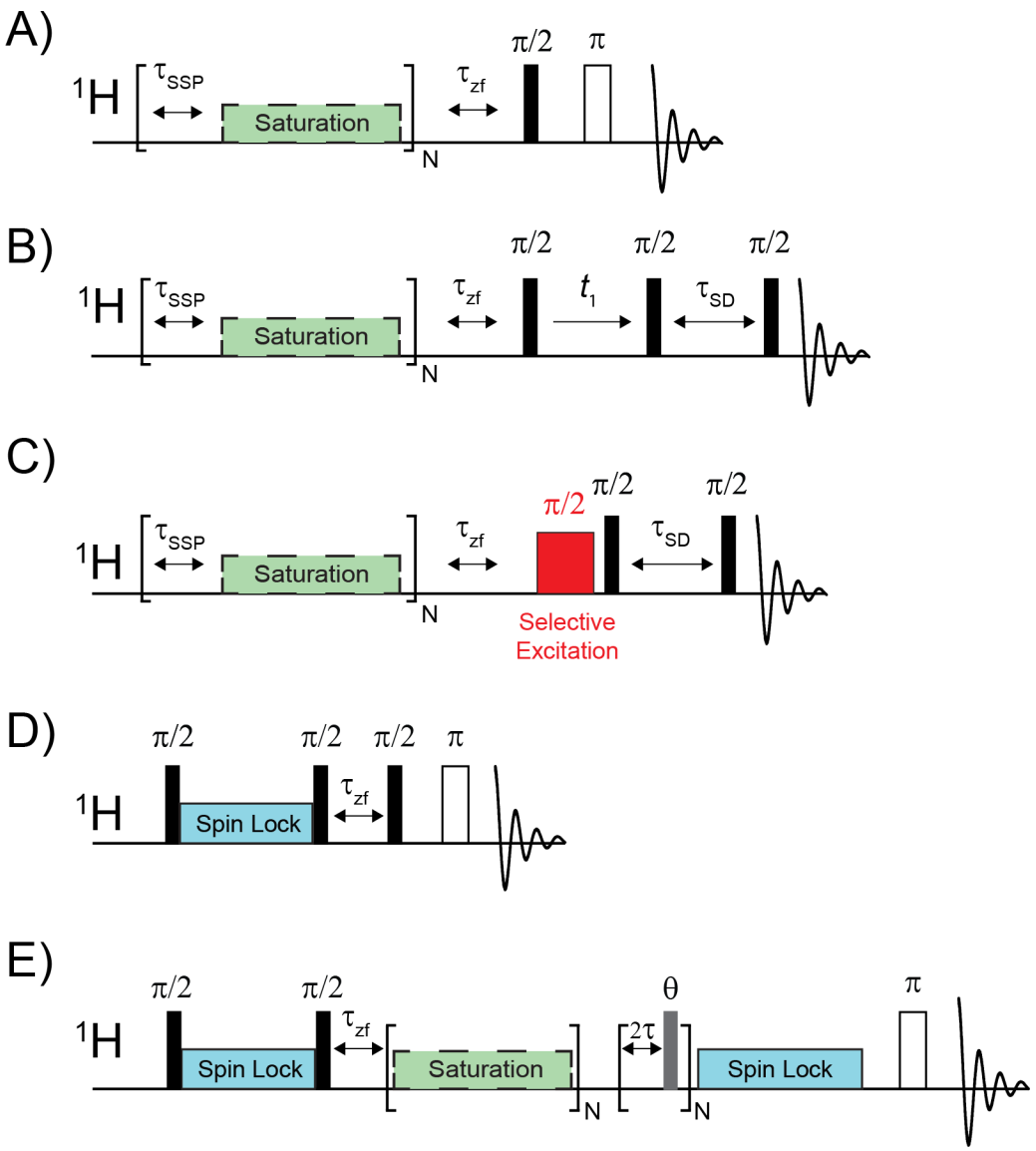

Figure S1. Diagrams of the pulse sequences used in this work. A) SSP optimization pulse sequence, B) 2D ^{1}H spin diffusion with SSP, C) 1D ^{1}H SE-SD, D) 1H spin echo with 1H spin-lock pulse to enhance longitudinal relaxation by ^{1}H spin diffusion and E) 1D SE-SD with spin-lock pulse to enhance ^{1}H longitudinal relaxation and DANTE SE pulse train. In each sequence, dashed green boxes indicate the optional inclusion of a selective saturation pulse (SSP). τ_{zf} denotes a *z*-filter delay that follows the final SSP. τ_{SSP} denotes a z-filter/spin diffusion delay in between the SSP.

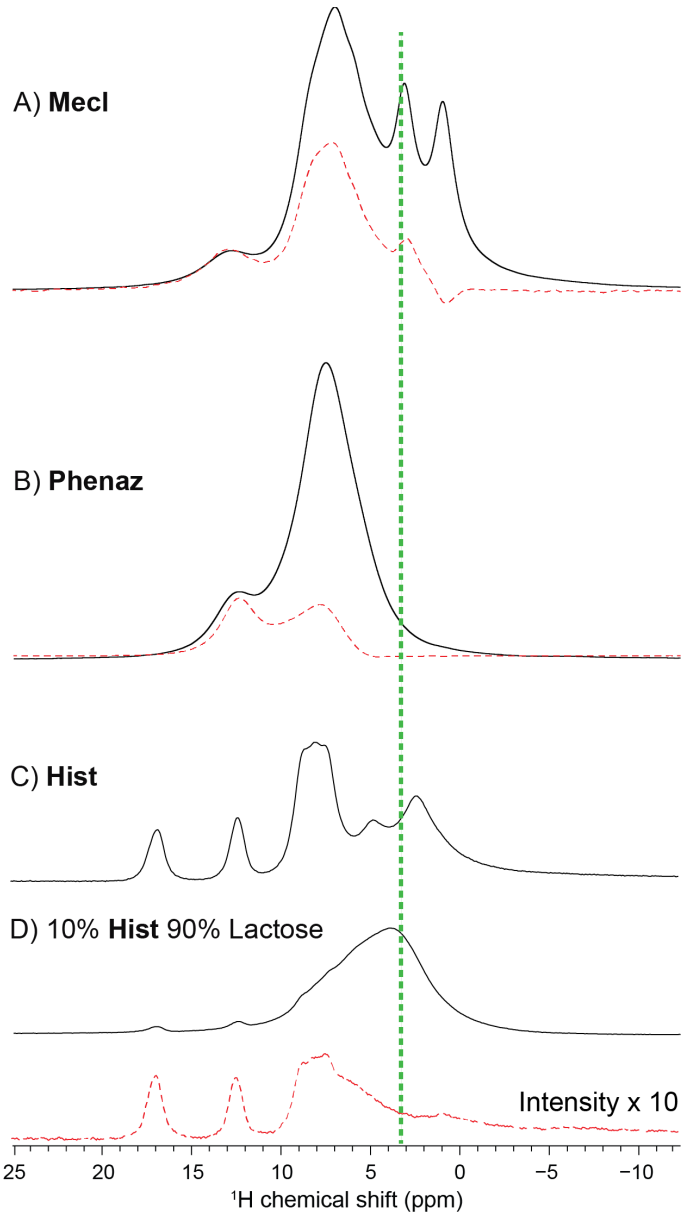

Figure S2. Comparison of ^{1}H spin echo solid-state NMR spectra obtained without (solid trace) or with a single 6 ms SSP (dashed trace) for A) **mecl**, B) **phenaz**, C) **hist** and D) a 10 wt-% **hist**, 90 wt-% **lactose** physical mixture. The SSP was applied at an offset of 3.5 ppm in all cases. **hist** is a convenient sample for the setup and optimization of SSPs, selective excitation pulses and 2D ^{1}H SD NMR experiments incorporating both elements. All spectra acquired at B_0 = 9.4 T with ν_{rot} = 50 kHz the pulse sequence shown in Figure S1A.

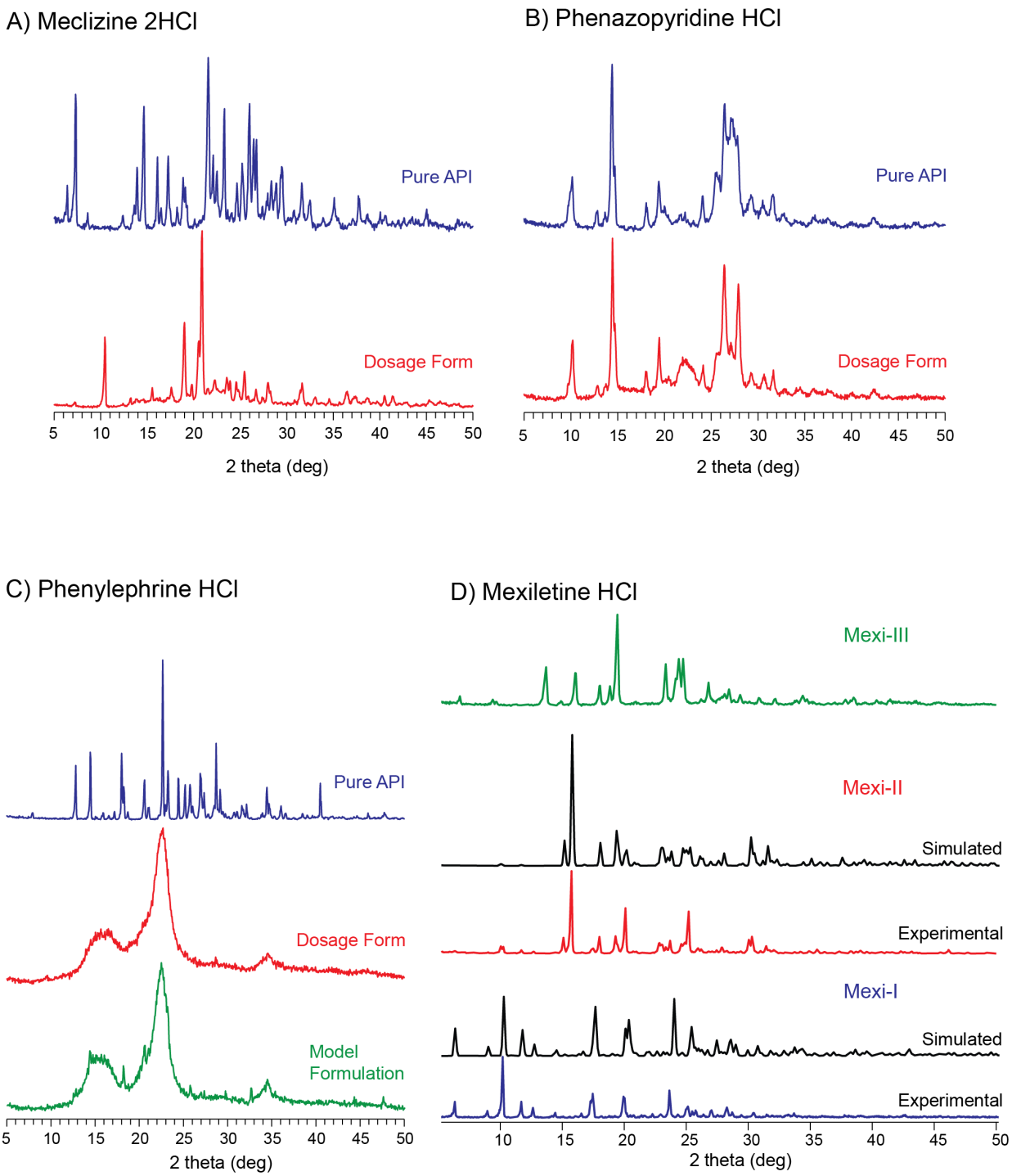

Figure S3. Experimental PXRD patterns for the samples used in this work. The simulated PXRD patterns for **mexi-I** and **mexi-II** were calculated from the previously reported single crystal X-ray diffraction structures (CSD codes: JIZJEH and JIZJEH01, respectively).

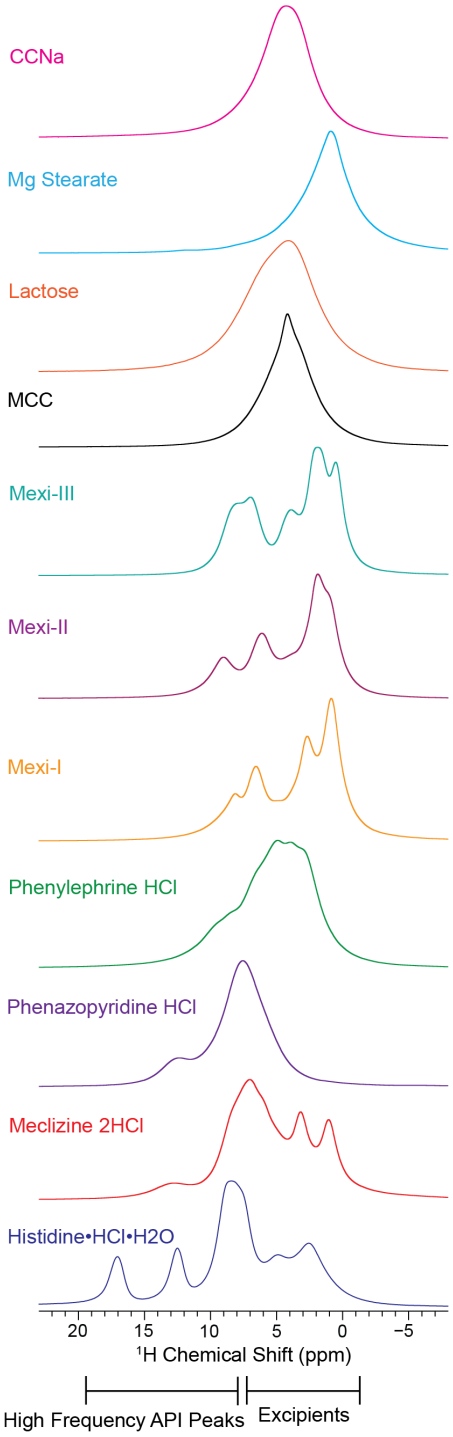

Figure S4. MAS ^{1}H spin-echo NMR spectra of commonly encountered excipients and the APIs studied in this work acquired at B_0 = 9.4 T with ν_{rot} = 50 kHz. CCNa is sodium croscarmellose and Mg Stearate is magnesium stearate. All other compounds are defined in Figure 1 of the main text.

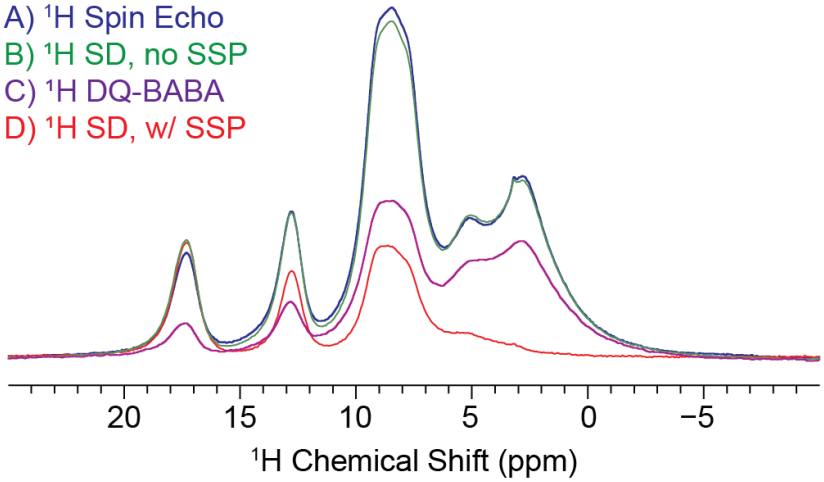

Figure S5. MAS ^{1}H SSNMR spectra of **hist** acquired with different pulse sequences A) spin echo, B) 2D ^{1}H SD without SSP, C) DQ-filtered spectrum obtained with the BABA pulse sequence and D) 2D ^{1}H SD obtained with a SSP applied at 3.5 ppm. For the 2D NMR experiments, the spectra were obtained from the first t_1 increment of the 2D experiment. The sensitivity of the high frequency feature at *ca.* 17 ppm is similar for all of the SQ experiments (A), B), and D)) but substantially decreased in the DQ experiment (C). All experiments were performed at B_0 = 9.4 T with ν_{rot} = 50 kHz.

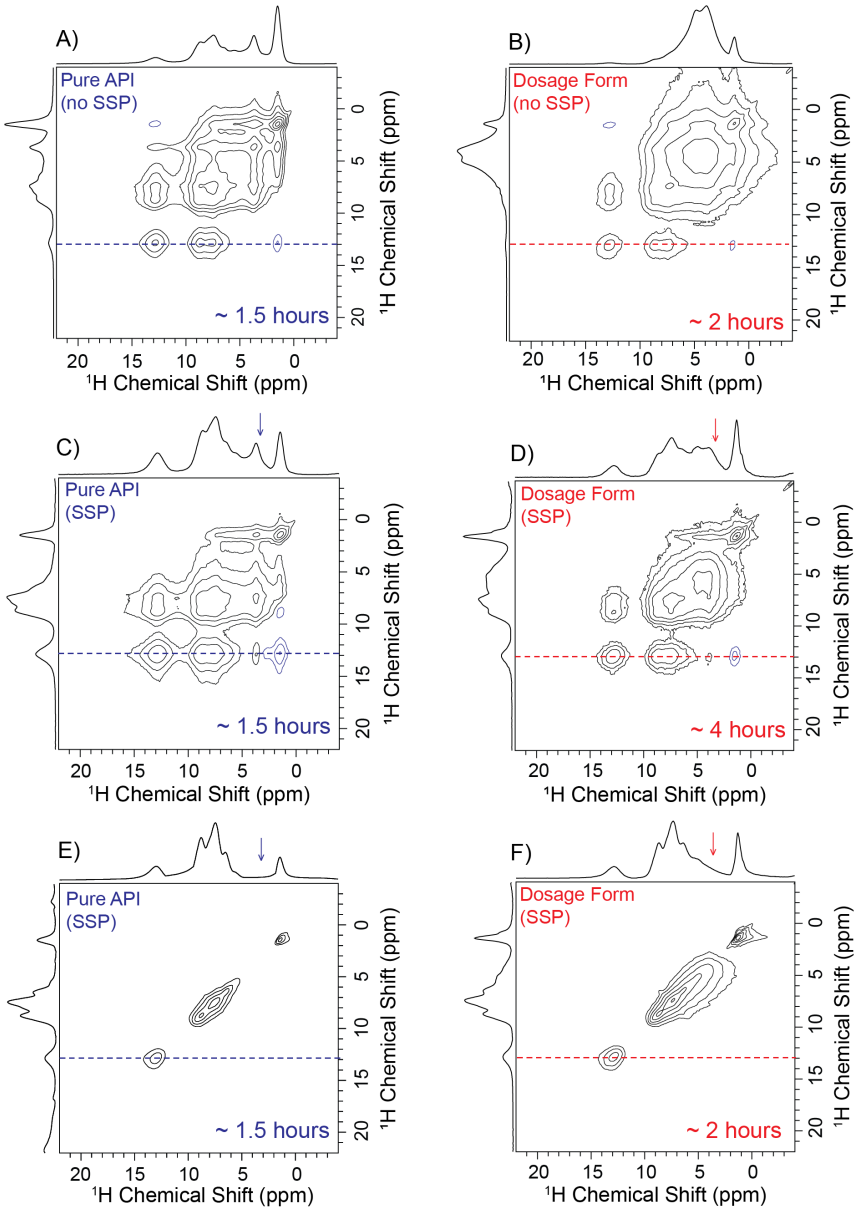

Figure S6. 2D ^{1}H SD NMR spectra of **mecl** pure (left column) and a commercial **mecl** tablet with 12.5 wt-% API (right column) acquired at B_0 = 18.8 T with ν_{rot} = 50 kHz. A) and B) acquired without SSP and with a 20 ms spin diffusion period, C) and D) acquired with a 6 ms SSP applied at 3.5 ppm and a 20 ms spin diffusion period. E) and F) were acquired with a 6 ms SSP applied at 3.5 ppm and no spin diffusion period. Rows indicated with the dashed lines are shown in Figure S7. Arrows indicate the frequency of the SSP. Total experiment times are indicated on the 2D NMR spectra.

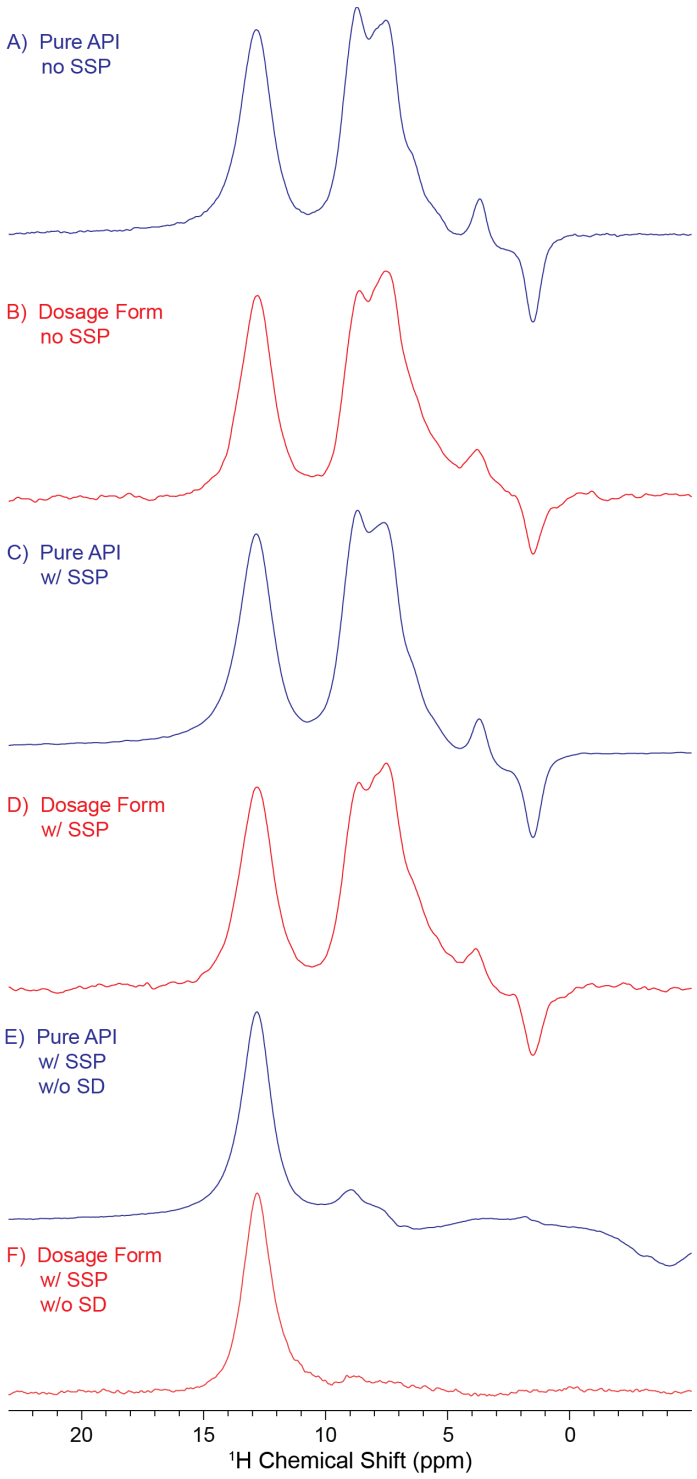

Figure S7. ^{1}H SSNMR spectra of **mecl** extracted from the indicated rows of the 2D SD ^{1}H NMR spectra shown in Figure S6. NMR spectra shown in (A-D) were acquired with 20 ms spin diffusion delay, while those in E) and F) were obtained without a diffusion delay.

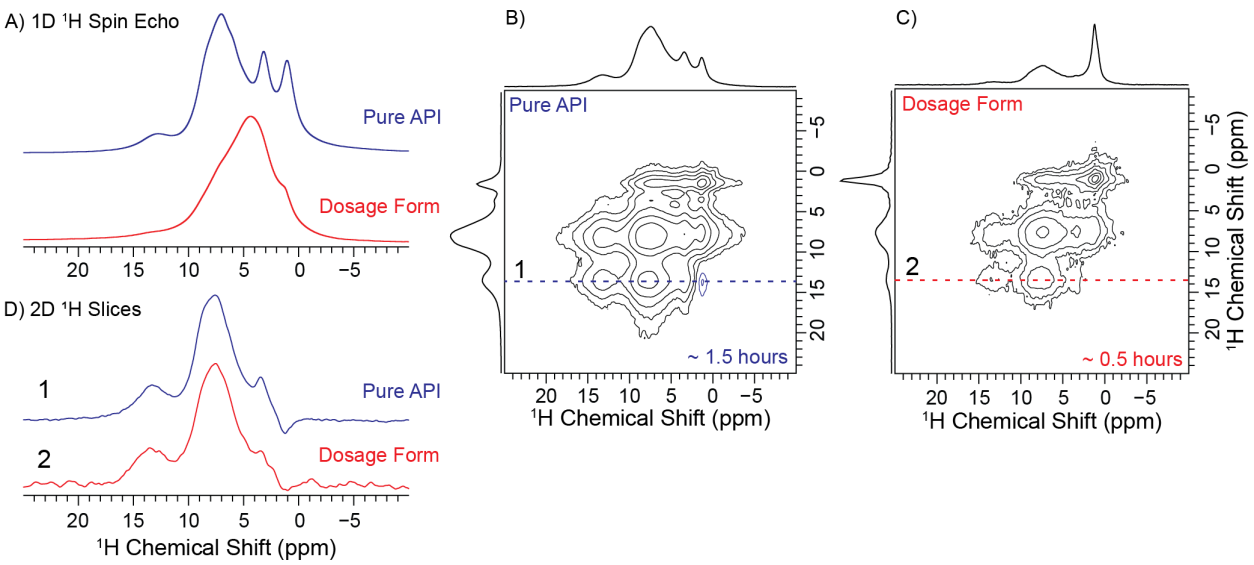

Figure S8. MAS ^{1}H SSNMR spectra of **mecl** pure and a commercial **mecl** tablet acquired at B_0 = 9.4 T with ν_{rot} = 50 kHz. A) 1D spin echo NMR spectra. B) and C) 2D ^{1}H SD NMR spectra acquired with a SSP applied at 3.5 ppm and a 20 ms spin diffusion period (see Figure S1 for the corresponding pulse sequence). D) 1D ^{1}H NMR spectra extracted from rows of the 2D NMR spectra, indicated with dashed lines.

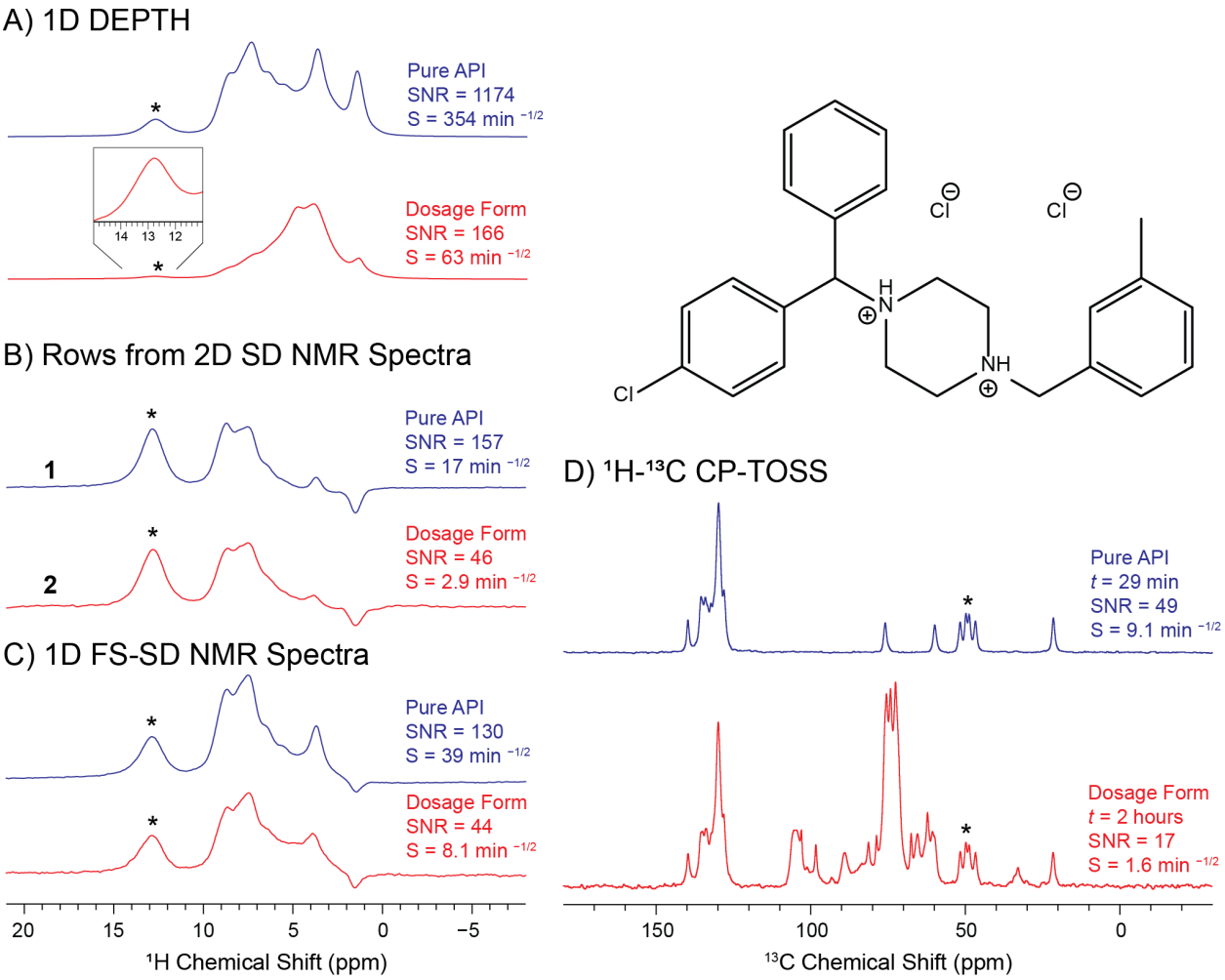

Figure S9. MAS ^{1}H and ^{1}H-^{13}C CP-TOSS SSNMR spectra of pure **mecl** (blue traces) and a **mecl** tablet (red traces). A) 1D DEPTH ^{1}H SSNMR spectra, B) ^{1}H SSNMR spectra extracted from rows of the 2D NMR spectra shown in Figure 2 of the main text, C) 1D SE-SD NMR SSNMR spectra, D) ^{1}H-^{13}C CP-TOSS. The sensitivities (S) and SNR ratios of the API signals are listed with each spectrum. The asterisks denote the peak used for determination of SNR and calculation of S. Note that because of signal overlap from multiple carbon atoms the aromatic ^{13}C NMR signals at *ca*. 130 ppm have much higher intensity, SNR and S than the NMR signal at 50 ppm used for determination of ^{13}C sensitivity (S = 5.8 min$^{-1/2}$ for the aromatic signals in the tablet). However, because of the peak overlap, the aromatic carbon NMR signals will likely not be diagnostic for different solid forms of **mecl**. Consequently, the second most intense and resolved ^{13}C NMR signal at *ca*. 50 ppm was used for the determination of ^{13}C sensitivity. ^{1}H SSNMR experiments were performed with 1.3 mm rotors, B_0 = 18.8 T and ν_{rot} = 50 kHz (left column). ^{1}H-^{13}C CP-TOSS SSNMR experiments were performed with 4.0 mm rotors, B_0 = 9.4 T and ν_{rot} = 8 kHz (right column).

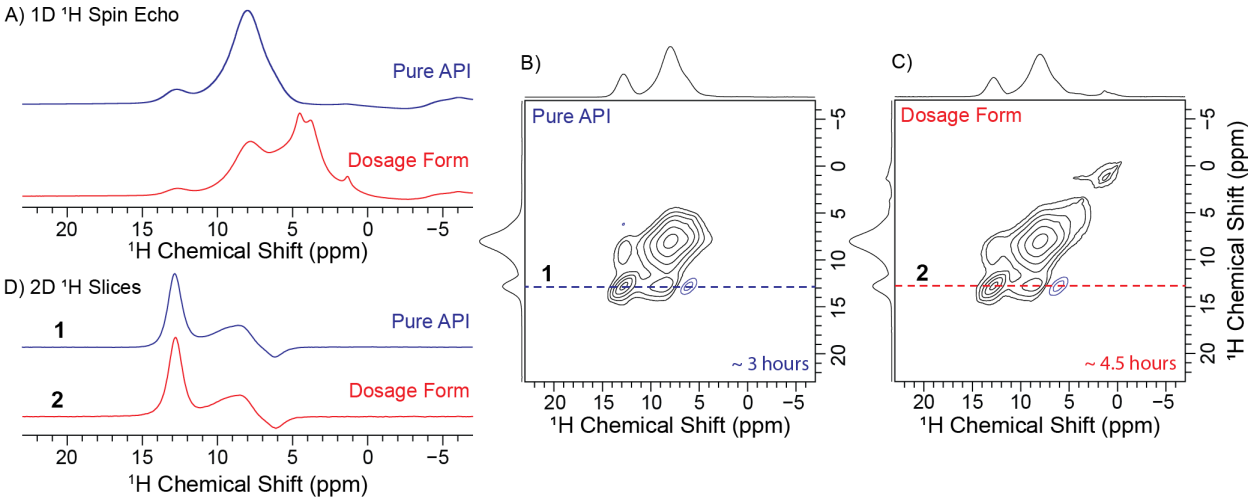

Figure S10. MAS ^{1}H SSNMR spectra of pure **phenaz** and a commercial **phenaz** tablet acquired at B_0 = 18.8 T with ν_{rot} = 50 kHz. A) 1D spin echo NMR spectra. B) and C) 2D ^{1}H SD NMR spectra acquired with a SSP applied at 3.5 ppm and a 20 ms spin diffusion time. D) ^{1}H SD NMR spectra extracted from the indicated rows of the 2D NMR spectra. Total experiment times are indicated on the 2D NMR spectra.

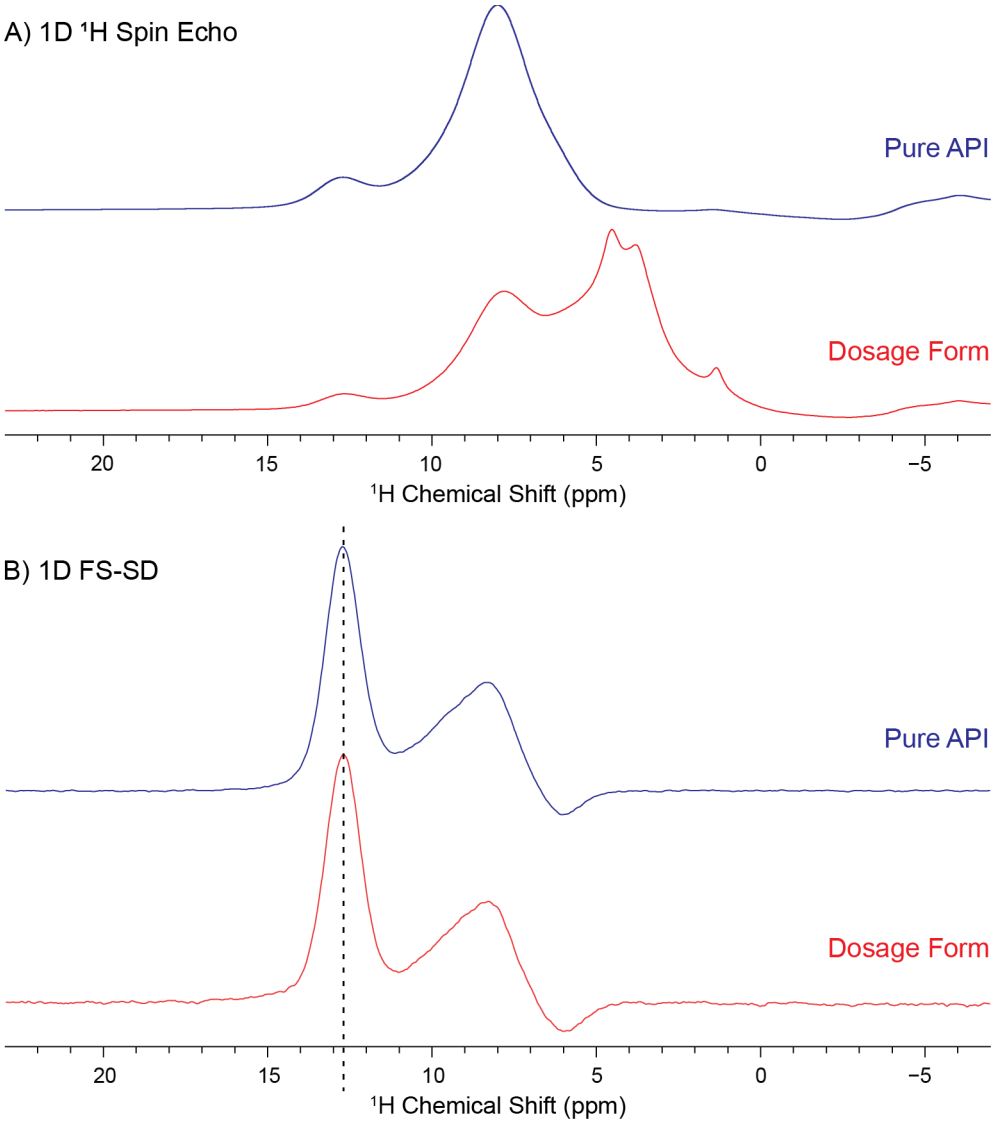

Figure S11. MAS ^{1}H SSNMR spectra acquired at B_0 = 18.8 T with ν_{rot} = 50 kHz of **phenaz** pure (blue traces) and a commercial **phenaz** tablet with 68-wt% API loading (red traces). A) ^{1}H spin echo SSNMR spectra. B) 1D SE-SD NMR spectra obtained with a 20 ms spin diffusion time. The dashed line indicates the transmitter position for the selective excitation pulse. The NMR spectrum of the **phenaz** tablet in B) was obtained in 4 minutes.

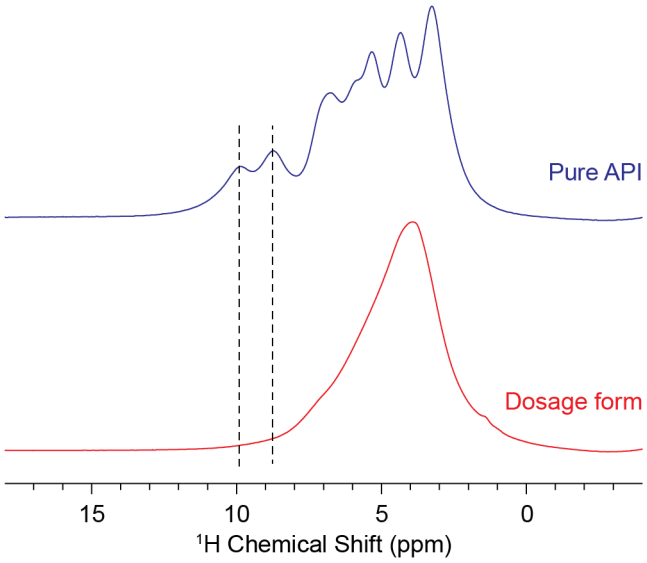

Figure S12. 1D ^{1}H MAS SSNMR spectra of **pheny** pure and a commercial **pheny** tablet. Both spectra were acquired at B_0 = 18.8 T with ν_{rot} = 50 kHz. Dashed lines indicate positions of the two features assigned to crystallographically-distinct ammonium protons in the pure material. These features are not visible in the spectrum of the dosage material likely because the API exists in a different solid phase in the tablet.

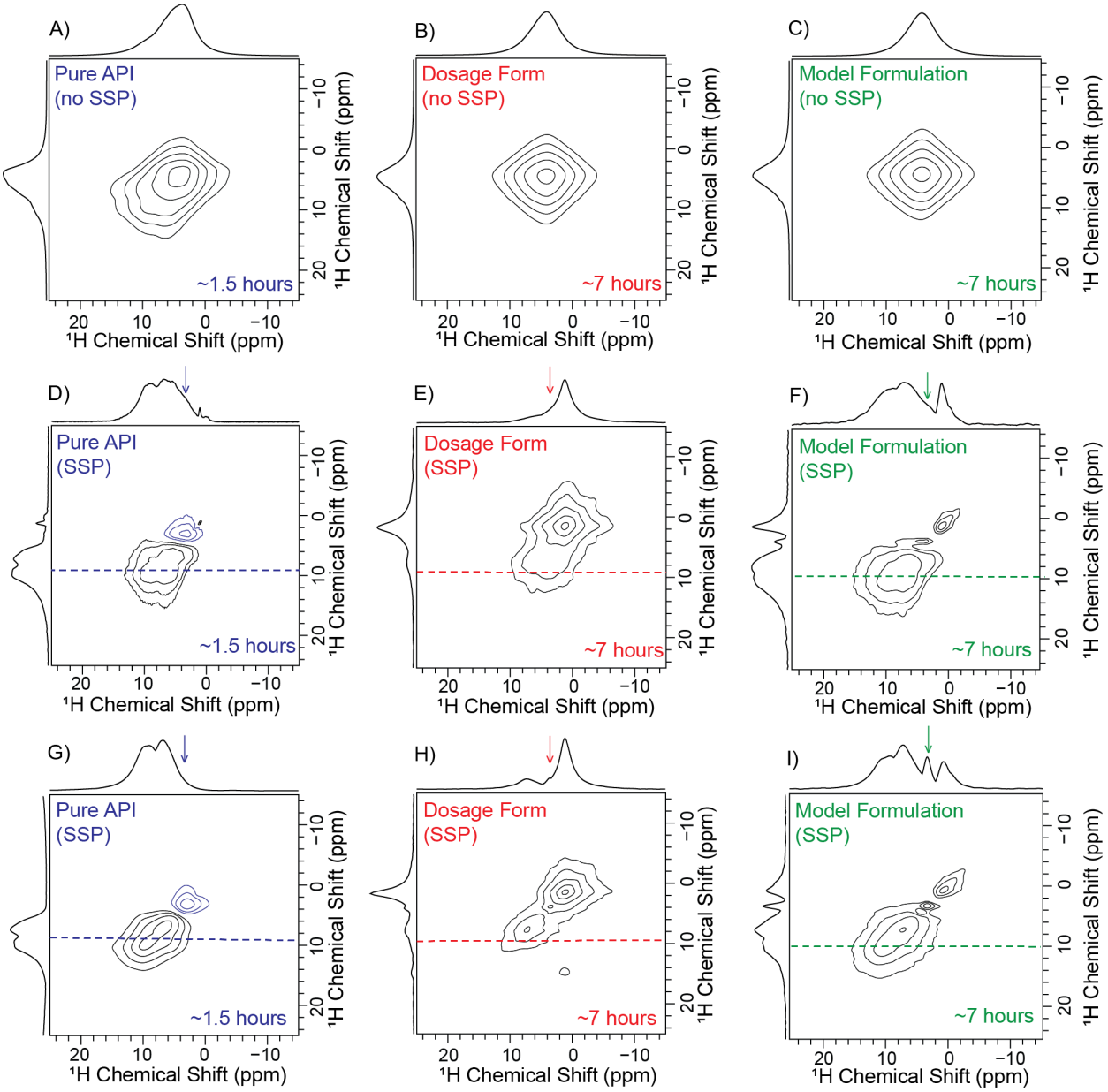

Figure S13. 2D ^{1}H SD NMR spectra of pure **pheny** (left column), a commercial 7 wt-% **pheny** tablet (middle column) and a model formulation consisting of a physical mixture of 7 wt-% **pheny** in **MCC** (right column). All spectra were acquired at B_0 = 9.4 T with ν_{rot} = 50 kHz. A), B) and C) acquired with 20 ms spin diffusion and no SSP D), E) and F) acquired with 20 ms spin diffusion and a 6 ms SSP applied at 4.5 ppm and G), H) and I) acquired with no spin diffusion period and a 6 ms SSP applied at 4.5 ppm. Rows indicated with the dashed lines are shown in Figure S14. The arrow indicates the transmitter offset of the SSP. Total experiment times are indicated on the 2D NMR spectra.

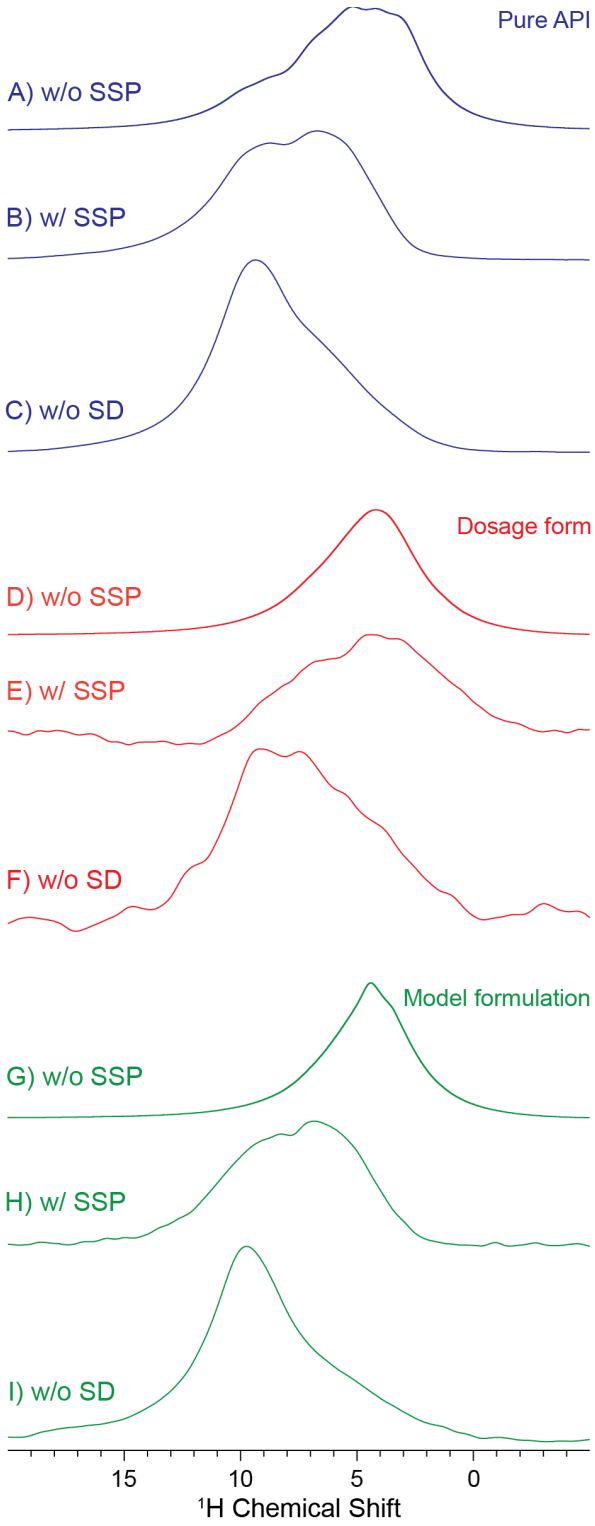

Figure S14. MAS ^{1}H SSNMR spectra of pure **pheny** (blue), commercial **pheny** tablet (red), and a model **pheny** formulation (green). A), D), and G) 1D ^{1}H spin echo NMR spectra. B), C), E), F), H) and I) 1D NMR spectra extracted from rows of the 2D ^{1}H SD NMR spectra were obtained at a 9.9 ppm chemical shift in the indirect dimension (Figure S13). All NMR spectra were acquired at B_0 = 9.4 T with ν_{rot} = 50 kHz.

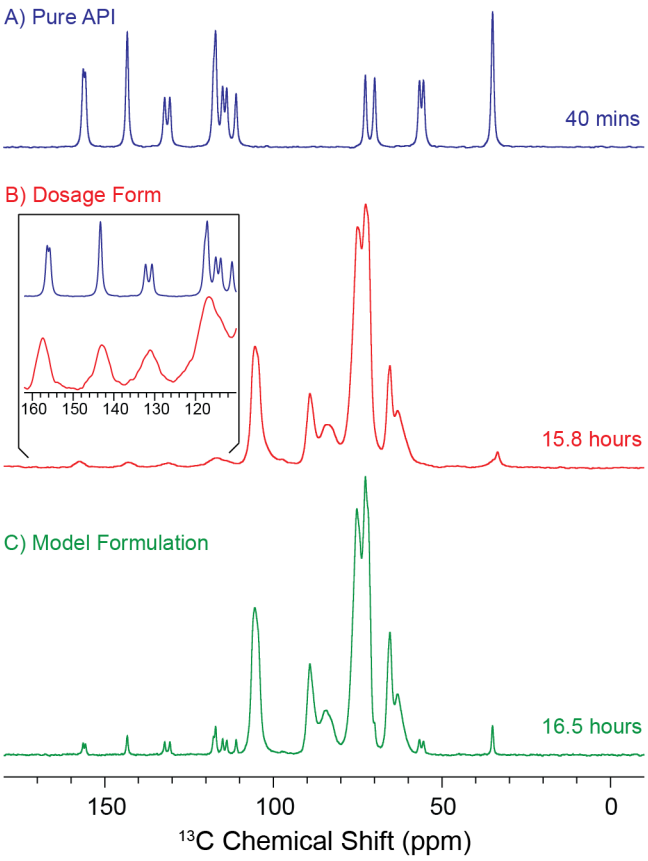

Figure S15. ^{1}H-^{13}C CP-TOSS/MAS spectra of A) pure **pheny**, B) a commercial **pheny** tablet with 7 wt-% API and C) a model formulation consisting of a physical mixture of 7 wt-% pure **pheny** and **MCC**. The inset in B) compares spectra of pure crystalline **pheny** and the commercial **pheny** tablet. All spectra were acquired with B_0 = 9.4 T, a 4.0 mm rotor and ν_{rot} = 8 kHz. Total experiment times are indicated. The ^{13}C SSNMR spectra suggest that the commercial tablet contains a different solid form of **pheny** that is clearly different from the crystalline pure form. The **pheny** in the tablet is likely amorphous.

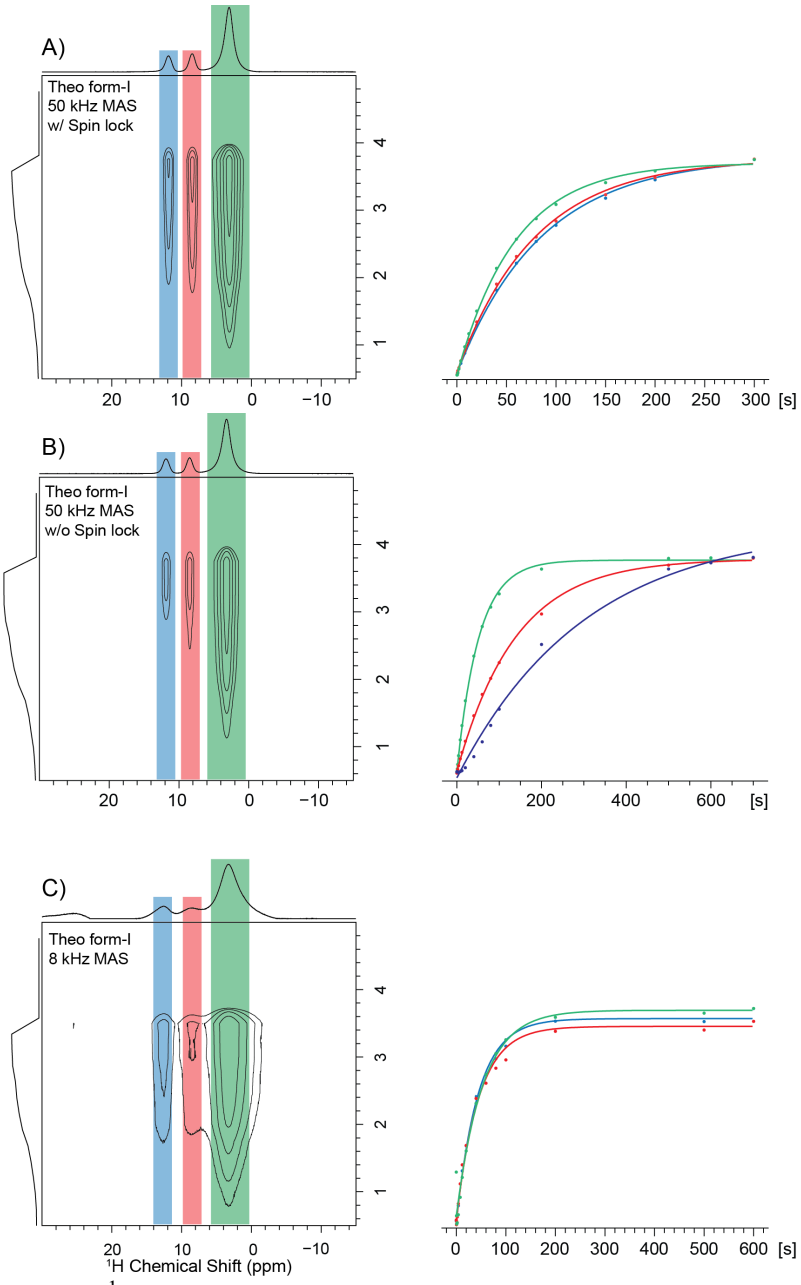

Figure S16. Summary of ^{1}H saturation recovery experiments on **theo-I**. Signal build-up plots are shown for the amine (NH, blue), methine (CH, red) and methyl (CH_3, green) protons of **theo-I**. The saturation recovery experiments were performed with A) 50 kHz MAS and a 1.8 ms spin-lock pulse to promote spin diffusion from methyl ^{1}H to the other ^{1}H, B) 50 kHz MAS without a spin-lock pulse and C) 8 kHz MAS. All experiments were performed with B_0 = 9.4 T. T_1 values determined form curve fits are shown in Tables S2 and S3.

Table S2. T_1 (^{1}H) measured for **theo-I** and **theo-II** with 8 kHz MAS

Polymorph	T_1 (s)		
	-NH	-CH	-CH_3
theo-I	45	45	53
theo-II	49	56	64

Table S3. T_1 (^{1}H) measured for **theo-I** and **theo-II** with 50 kHz MAS

Polymorph	T_1(s)[a]			T_1 w/ ^{1}H spin-lock (s)[b]		
	-NH	-CH	-CH_3	-NH	-CH	-CH_3
theo-I	303	139	52	85	78	59
theo-II	463	109	61	73	72	65

[a]Measured with a standard saturation recovery pulse sequence.
[b]Measured with a 1.8 ms ^{1}H spin-lock pulse inserted prior to the final excitation pulse in a saturation recovery pulse sequence (pulse sequence similar to that depicted in Figure S1D). The ^{1}H spin-lock pulse promotes spin diffusion between the methyl ^{1}H and high frequency amine and methine ^{1}H spins, resulting in a reduction in the apparent T_1 of the amine and methine.

Table S4. Data used for the calibration plot in Figure 7 of the main text.

theo-II wt. (%)	Integrated Intensity	Predicted theo-II wt.%[a]	Absolute wt.% Error (wt. %)	Percentage Error (%)
2	1.54	1.50	0.50	24.9
4	4.02	3.92	0.08	1.98
6.1	6.89	6.72	0.62	10.1
9.8	9.80	9.55	0.25	2.55
			Average = 0.36 wt.%	Average = 9.9 %

[a] The predicted theo-II wt.% was calculated using the equation from the calibration curve:

Predicted wt.% = (Integrated Intensity)/1.03.

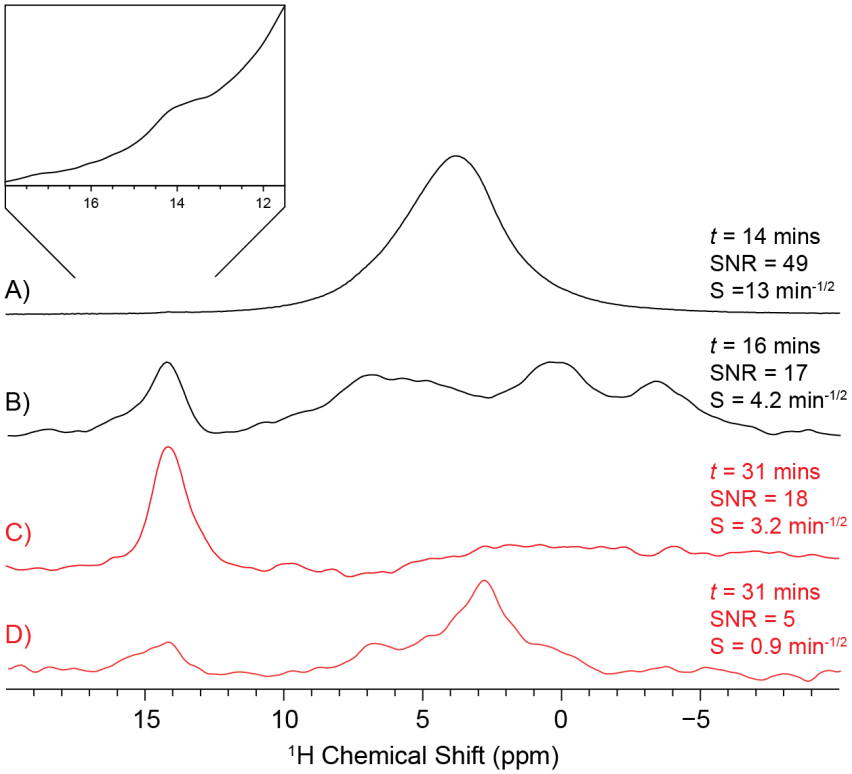

Figure S17. ^{1}H SSNMR spectra of a physical mixture of 98 wt% **MCC** and 2 wt% **theo-II**. ^{1}H spin echo spectrum recorded (A) without and (B) with SSP on resonance with **MCC**. (C, D) 1D SE-SD ^{1}H SSNMR spectra with the DANTE excitation pulse on resonance with the high frequency amine ^{1}H NMR signal of **theo-II**. The 1D SE-SD spectrum in (C) was recorded with a 20 μs spin-lock pulse to minimize ^{1}H spin diffusion. The 1D SE-SD spectrum in (D) was obtained with a 1.8 ms spin-lock pulse following the SE DANTE pulse to promote ^{1}H spin diffusion. ^{1}H SSNMR spectra were obtained with a 50 kHz MAS frequency at B_0 = 9.4 T.

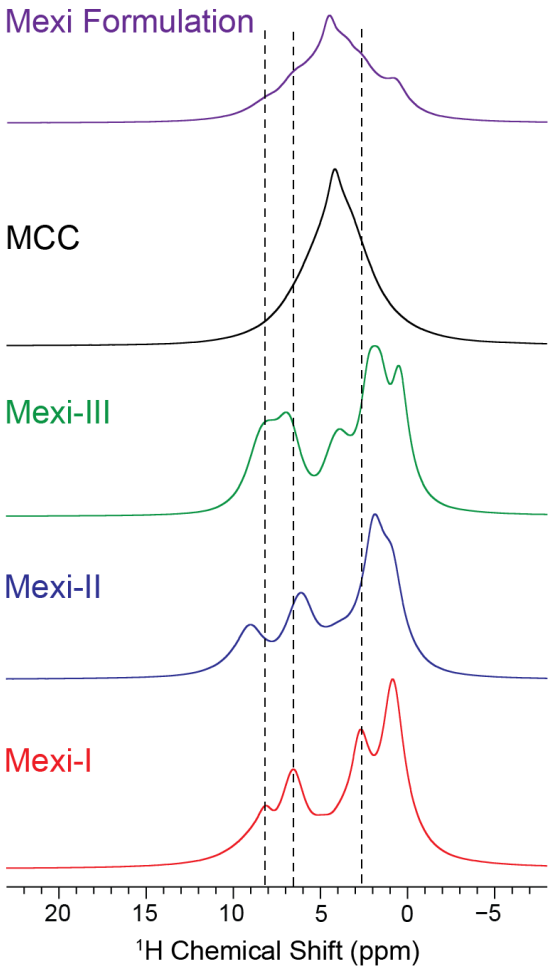

Figure S18. MAS ^{1}H spin-echo NMR spectra of the three **mexi** polymorphs, **MCC** and the model **mexi** formulation acquired at B_0 = 9.4 T with ν_{rot} = 50 kHz. Vertical lines are guides for the eye to illustrate differences in isotropic ^{1}H chemical shifts.

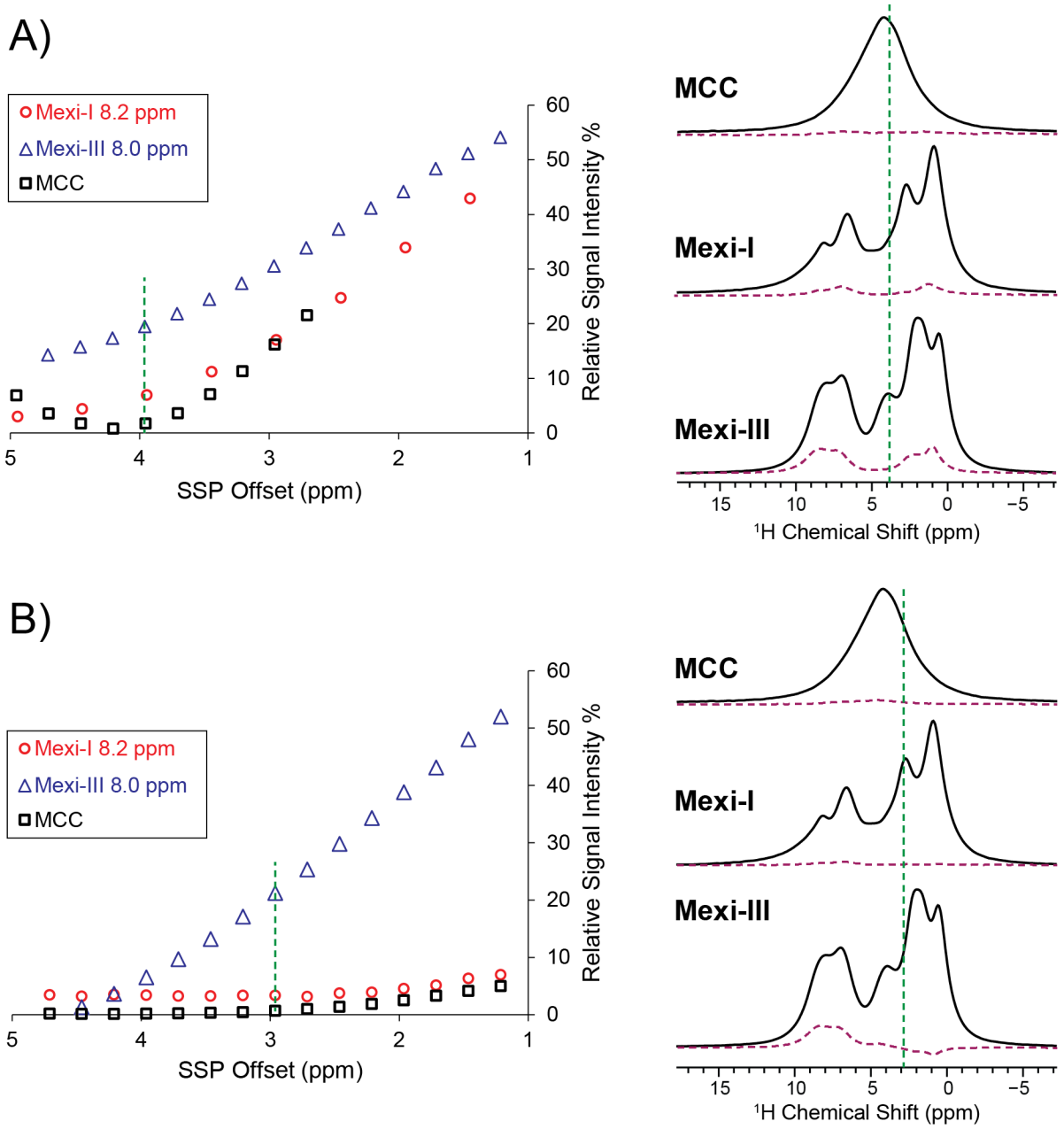

Figure S19. Optimization of SSP conditions on **mexi-I**, **mexi-III** and **MCC**. The plots show the relative signal intensities as a function of the SSP offset. For **mexi-I** and **mexi-III** only the relative signal intensity of the ammonium ^{1}H signal with the highest chemical shift is plotted. A) A single 6 ms SSP was applied with a 20 μs z-filter delay preceding the spin echo. ^{1}H NMR spectra are shown without any SSP (solid trace) and with an SSP offset of 3.95 ppm (dashed trace). B) Three 6 ms SSP were applied, with a 20 ms delay (τ_{SSP}) in between each SSP and a 20 μs z-filter delay preceding the spin echo. ^{1}H NMR spectra are shown without any SSP (solid trace) and with three SSP applied at an offset of 2.9 ppm (dashed trace). The vertical dashed lines indicate the SSP offset. All data acquired at B_0 = 9.4 T with ν_{rot} = 50 kHz with the pulse sequence shown in Figure S1A.

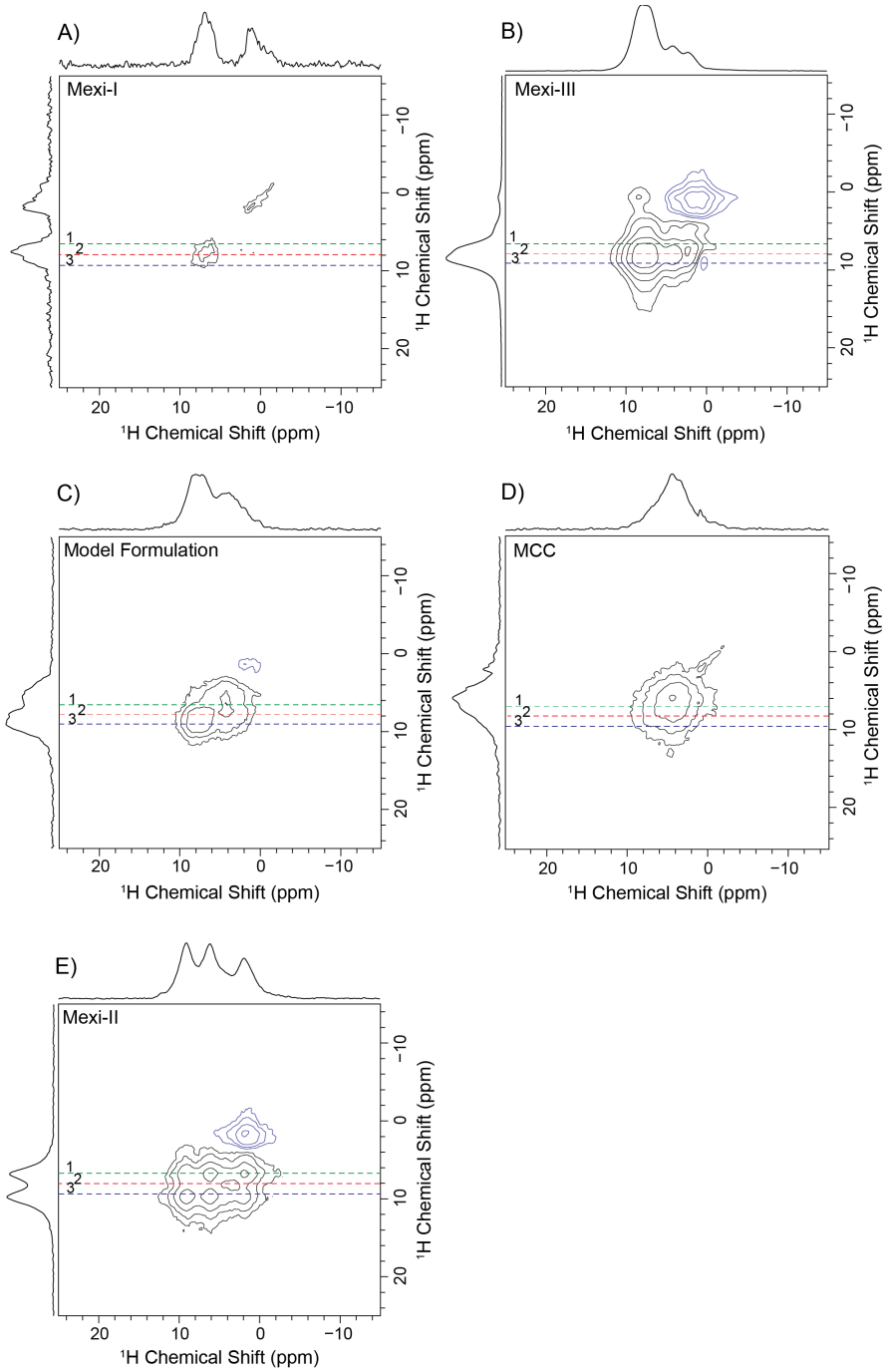

Figure S20. 2D ^{1}H SD NMR spectra acquired at B_0 = 9.4 T with ν_{rot} = 50 kHz. A) **mexi-I**, B) **mexi-III**, and C) a model formulation, D) **MCC** and E) **mexi-II**. The model formulation is a physical mixture of 5.2 wt-% **mexi-III**, 26.7 wt-% **mexi-I**, and 68.0 wt-% **MCC** (total API load of 32 wt-%). Three SSPs were applied at an offset of 2.9 ppm with a spin diffusion period of 20 ms separating each SSP. This SSP condition saturates **mexi-I** and the **MCC**, allowing the ^{1}H SSNMR signals from **mexi-III** to be selectively detected in the model formulation (see Figure S19). Different rows extracted from the 2D SD ^{1}H NMR spectra are compared in Figure S21 and Figure 6 of the main text.

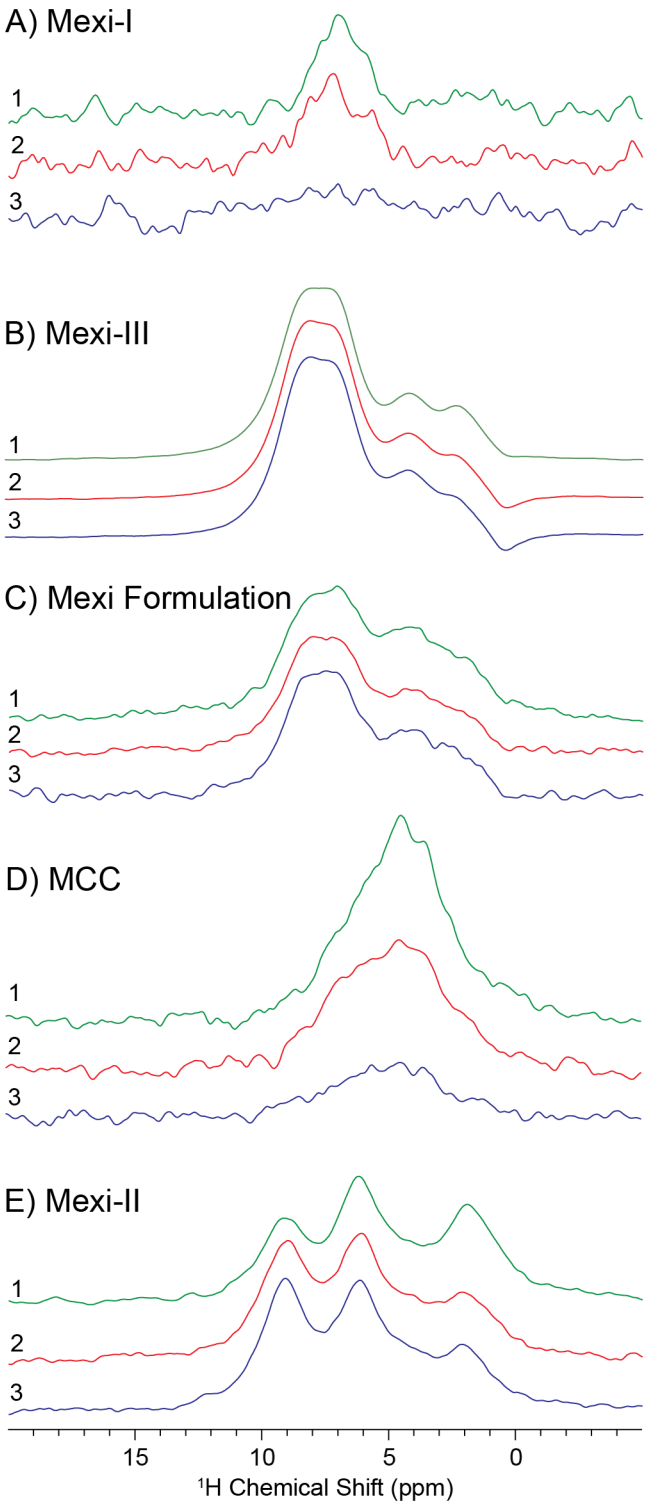

Figure S21. Comparison of rows extracted from the 2D SD ^{1}H NMR spectra of the different **mexi** forms. The corresponding 2D NMR spectra are shown in Figure S20. Rows 1, 2 and 3 were extracted from indirect dimension chemical shifts of 6.8 ppm, 8.0 ppm and 9.7 ppm. Figure 6 of the main text compares the 9.7 ppm rows for the different samples.

Table S5. ^{1}H Longitudinal Relaxation Time Constants (T_1)* for Different Samples

Sample	T_1 (s)	Magnetic Field (T)
pure **mecl**	7.6	18.8
pure **mecl**	5.3	9.4
mecl tablet	5.3	18.8
pure **phenaz**	7.0	18.8
phenaz tablet	12	18.8
pure **phenaz**	10.4	9.4
phenaz tablet	22	9.4
pure **pheny**	18	9.4
pheny model formulation	15	9.4
pure **mexi-I**	6.3	9.4
pure **mexi-II**	4.6	9.4
pure **mexi-III**	1.5	9.4

*The T_1 is reported for the ^{1}H signal with the highest chemical shift.

References

(1) Hildebrand, M.; Hamaed, H.; Namespetra, A. M.; Donohue, J. M.; Fu, R.; Hung, I.; Gan, Z.; Schurko, R. W. *CrystEngComm* **2014**, *16*, 7334.

(2) Namespetra, A. M.; Hirsh, D. A.; Hildebrand, M. P.; Sandre, A. R.; Hamaed, H.; Rawson, J. M.; Schurko, R. W. *CrystEngComm* **2016**, *18*, 6213–6232.

(3) Pinon, A. C.; Rossini, A. J.; Widdifield, C. M.; Gajan, D.; Emsley, L. Polymorphs of Theophylline Characterized by Dnp Enhanced Solid-State Nmr. *Mol. Pharm.* **2015**, *12*, 4146-4153

(4) Harris, R. K.; Becker, E. D.; Cabral de Menezes, S. M.; Granger, P.; Hoffman, R. E.; Zilm, K. W. *Pure Appl. Chem.* **2008**, *80*, 59–84.

(5) Cory, D. .; Ritchey, W. . *J. Magn. Reson.* **1988**, *80*, 128–132.

(6) Song, Z.; Antzutkin, O. N.; Feng, X.; Levitt, M. H. *Solid State Nucl. Magn. Reson.* **1993**, *2*, 143–146.

(7) Antzutkin, O. N. *Prog. Nucl. Magn. Reson. Spectrosc.* **1999**, *35*, 203–266.

(8) Fung, B. M.; Khitrin, A. K.; Ermolaev, K. *J. Magn. Reson.* **2000**, *142*, 97–101.